Transient brain networks underlying interpersonal strategies during synchronized action

Ole Adrian Heggli, [iD][1] Ivana Konvalinka,[2] Joana Cabral,[3,4] Elvira Brattico,[1,5] Morten L. Kringelbach,[1,4] and Peter Vuust[1]

[1]Center for Music in the Brain, Aarhus University & The Royal Academy of Music Aarhus/Aalborg, Aarhus, Denmark, [2]SINe Lab, Section for Cognitive Systems, DTU Compute, Technical University of Denmark, Kongens Lyngby, Denmark, [3]Life and Health Sciences Research Institute (ICVS), School of Medicine, University of Minho, Braga, Portugal, [4]Department of Psychiatry, University of Oxford, Oxford, UK, and [5]Department of Educational Sciences, Psychology, Communication, University Aldo Moro of Bari, Italy

Correspondence should be addressed to O.A. Heggli, Center for Music in the Brain, Department of Clinical Medicine, Aarhus University, Nørrebrogade 44, Building 1A Office 1-12, 8000 Aarhus, Denmark. E-mail: ole.heggli@clin.au.dk.

Abstract

Interpersonal coordination is a core part of human interaction, and its underlying mechanisms have been extensively studied using social paradigms such as joint finger-tapping. Here, individual and dyadic differences have been found to yield a range of dyadic synchronization strategies, such as mutual adaptation, leading–leading, and leading–following behaviour, but the brain mechanisms that underlie these strategies remain poorly understood. To identify individual brain mechanisms underlying emergence of these minimal social interaction strategies, we contrasted EEG-recorded brain activity in two groups of musicians exhibiting the mutual adaptation and leading–leading strategies. We found that the individuals coordinating via mutual adaptation exhibited a more frequent occurrence of phase-locked activity within a transient action–perception-related brain network in the alpha range, as compared to the leading–leading group. Furthermore, we identified parietal and temporal brain regions that changed significantly in the directionality of their within-network information flow. Our results suggest that the stronger weight on extrinsic coupling observed in computational models of mutual adaptation as compared to leading–leading might be facilitated by a higher degree of action–perception network coupling in the brain.

Key words: musical interaction; interpersonal synchronization; functional connectivity; EEG

Introduction

Humans are inherently social, as evident across a wide range of social behaviours and the importance we place on social interactions. In fact, many of the conditions we deem psychiatric disorders, such as autism or social anxiety disorder, manifest as abnormal social functioning (Young, 2008; Schilbach *et al.*, 2013, 2016; Bolis *et al.*, 2017). Recently, theoretical and technological advances in behavioural and brain science have made it possible to study social interaction not in isolation, but rather within a framework assuming multiple interacting agents (Frith, 2007; Koban *et al.*, 2017; Redcay and Schilbach, 2019). A particularly important aspect of social interaction is interpersonal synchronization, defined as the adjustment of rhythmical movements

or actions based on interaction with each other. Interpersonal synchronization affects not only how we interact but also how we perceive and relate to other people (Hove and Risen, 2009; Cirelli *et al.,* 2014; Stupacher *et al.,* 2017a,b). This type of synchronization can emerge spontaneously, such as in the tendency for synchronized behaviour in walking, joke telling and general body movements, or with intention, such as in musical performance or dance (Richardson *et al.,* 2007; van Ulzen *et al.,* 2008; Schmidt *et al.,* 2014; Stupacher *et al.,* 2017a). In recent work, we have shown how interpersonal dynamics in synchronization tasks can be modelled using a network of coupled oscillators (Heggli *et al.,* 2019a). We proposed that interpersonal synchronization strategies such as mutual adaptation, leading–following and leading–leading rely on action–perception links modulated by individual decisions to integrate or segregate information related to self-produced actions and the perception of other-produced actions (Milward and Sebanz, 2016; Novembre *et al.,* 2016; Koban *et al.,* 2017; Heggli *et al.,* 2019a). While there has been a considerate amount of research on the nature of these types of interpersonal synchronization strategies, we know little about the underlying neural mechanisms (Konvalinka and Roepstorff, 2012; Koban *et al.,* 2017).

Joint finger-tapping paradigms offer a controlled, minimalistic approach to study intentional interpersonal synchronization. Here, participants are paired in dyads and are asked to tap a simple rhythm together, with the task to 'maintain the tempo and synchronize' (Konvalinka *et al.,* 2010; Gebauer *et al.,* 2016; Heggli *et al.,* 2019b). Despite the relative simplicity of such a paradigm, complex dyadic dynamics can be observed during the interaction, in particular, in the way participants adjust their tapping to each other. This can be measured by calculating lagged cross-correlation coefficients between the interacting participants' intertap intervals. This is shown in Figure 1A, where cross-correlation coefficients at lag −1, lag 0 and lag +1 create characteristic lag patterns during synchronized interaction. These patterns and in particular the balance between lag −1 and lag +1 are indicative of the synchronization strategy. The most prominent synchronization strategy, mutual adaptation, emerges when the participants mutually and continuously adjust their upcoming tap based on the other's previous tap (Konvalinka *et al.,* 2010; Gebauer *et al.,* 2014). This results in a positive correlation at both lag +1 and lag −1, and usually a negative correlation at lag 0, indicating that the participants' intertap intervals oscillate reciprocally around each other (Konvalinka *et al.,* 2010). Leading–following occurs when one participant unilaterally decides to decouple from the other, placing more importance on maintaining their own accuracy and stability than the collective synchronization (Konvalinka *et al.,* 2014). These two synchronization strategies have been reported across multiple studies, with mutual adaptation being the most common to emerge when participants have the same task constraints (Kung *et al.,* 2013; Konvalinka *et al.,* 2014; Gebauer *et al.,* 2016). Recently, a third interpersonal synchronization strategy, 'leading–leading', was reported in musicians (Heggli *et al.,* 2019b). Leading–leading is characterized by a weakly positive correlation at all three lags, indicating that there is little to no adaptation between the dyad members. Resisting adaptation is a general characteristic of leaders in joint finger-tapping (Fairhurst *et al.,* 2014; Konvalinka *et al.,* 2014). These synchronization strategies, like many aspects of human social interaction, are likely dynamic in their nature. However, due to the short trials (10 s) in the current experiment, and the need for multiple finger taps to establish a lag pattern, here we treat them as stationary (Konvalinka *et al.,* 2014).

Previous neurophysiology research has shown that leaders and followers in coupled interaction can be distinguished by a stronger suppression of frontal alpha activity in EEG among leaders; interbrain synchronization across alpha, beta and gamma band oscillations during imitation tasks; and differences in patterns of directed inter-brain coupling (Dumas *et al.,* 2010; Sänger *et al.,* 2013; Konvalinka *et al.,* 2014). However, research on symmetric interaction dynamics has in general been focused on finding neural differences between synchronized and non-synchronized behaviour, rather than differences in synchronization strategies (Tognoli *et al.,* 2007; Dumas *et al.,* 2019). For instance, suppression of the mu rhythm has been linked to dyadic synchronization levels, and a right centroparietal oscillatory component termed the phi complex has been proposed to reflect the partner's influence on produced actions in dyadic interactions (Tognoli *et al.,* 2007; Fitzpatrick *et al.,* 2019). While many of these studies report effects in the alpha frequency band, there is also evidence for the involvement of beta frequency band in interpersonal synchronization. For instance, in-phase transcranial alternating current stimulation over the left motor cortex at 20 Hz across interacting dyads enhanced behavioural synchronization in a joint finger-tapping task (Novembre *et al.,* 2017). Taken together these studies indicate involvement of multiple complementary mechanisms in dyadic synchronization.

In this exploratory study, we aimed to identify differences in neural mechanisms across alpha and beta band frequencies related to interpersonal synchronization strategies in musicians. We used a dual-EEG dataset based on a recent joint finger-tapping experiment, wherein the interacting musicians exhibited either a leading–leading or mutual adaptation synchronization strategy (for behavioural results, see Heggli *et al.,* 2019b). Here, our approach was to investigate how within-brain processes are modulated by interpersonal behaviour. We used a connectivity-centred approach where we analyzed how different areas of the brain dynamically form temporal networks exhibiting coherent activity. In this framework, cognition is thought to involve a coordinated integration of information between brain areas, through metastable networks that collectively form a repertoire of brain states (Cabral *et al.,* 2014; Deco *et al.,* 2015; Lord *et al.,* 2019). Such functional networks have been observed across neuroimaging modalities, both during rest and in active tasks (Deco *et al.,* 2011). To identify time-varying and transient brain networks related to synchronization strategies, we adapted the recently developed Leading Eigenvector Dynamics Analysis (LEiDA) method (Cabral *et al.,* 2017). This method captures instantaneous phase-locking patterns (PL states) in the EEG signal and uses a clustering algorithm to identify recurrent PL states that consistently occur across all participants. Following the identification of PL states, we can identify between-group differences by statistically quantifying the group-dependent occurrence probabilities of PL states. To further distinguish differences in neural mechanisms between synchronization strategies, we also calculated directed phase transfer entropy (dPTE), a measurement of information flow between brain regions (Hillebrand *et al.,* 2016). This approach hence allows for identifying both how the leading–leading and mutual adaptation synchronization strategies differ in terms of the occurrence probability of functional brain networks and the information flow within networks. By employing these two complementary data-driven approaches, we investigated the differences in brain networks between dyads mutually adapting to each other and the mutually non-adaptive dyads (leading–leading). We use these differences to infer brain networks involved in self–other integration.

(A) Overview of joint finger tapping paradigm
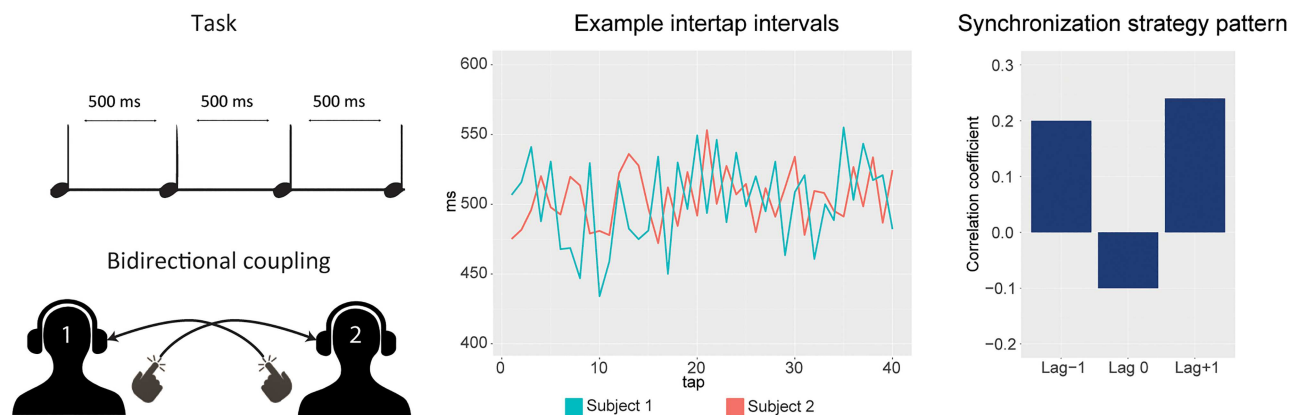
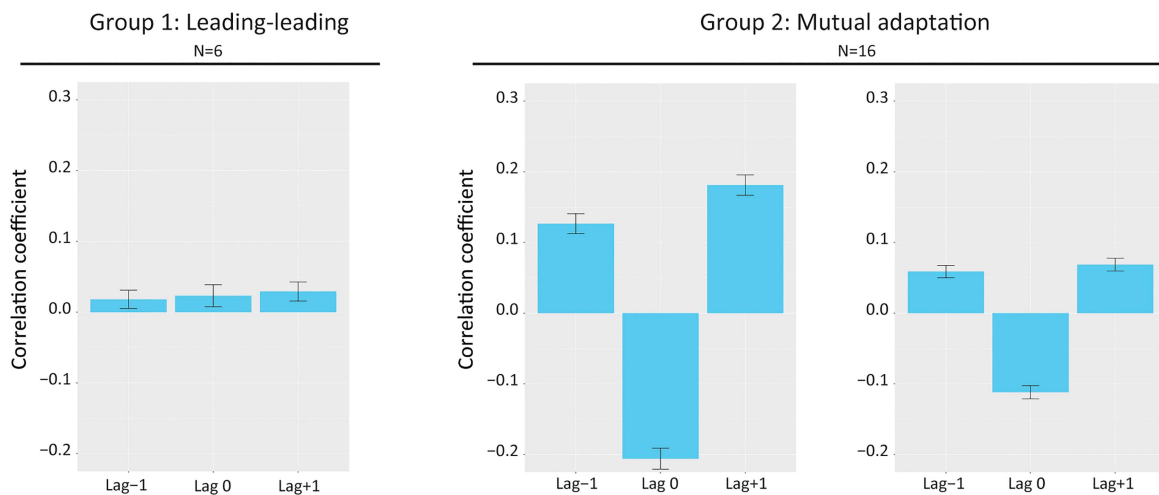
(B) Group synchronization strategy

Fig. 1. Overview of the paradigm and behavioural data. In (A), a joint finger-tapping paradigm is illustrated. Two participants tap together, in a bidirectionally coupled setting so that dyad member 1 hears dyad member 2, and vice versa. For the data used in the study, all trials had a target intertap interval (ITI) of 500 ms. Their resulting time series of intertap intervals is then cross-correlated at lag −1, lag 0 and lag +1. The pattern from this correlation indicates synchronization strategy. In (B), we show the behavioural results from the data used in this study. Here, N signifies the included participants in each group. One subset of participants, consisting primarily of drummers paired with drummers exhibited a leading–leading strategy, here shown on the left in group 1. The two other significantly different subsets of participants both exhibited a mutual adaptation strategy, with differing strengths in the pattern. For further details, see Heggli *et al.* (2019b). For this study, we collated the two instances of mutual adaptation, shown here on the right as group 2.

Methods

The behavioural results of the experiment presented here have been previously reported in Heggli *et al.* (2019b). For clarity, a brief description of the participants, protocol and behavioural results is included below.

Ethics statement

The experiment was conducted at the Center for Music in the Brain, Department of Clinical Medicine at Aarhus University, Denmark. Ethical approval was governed by the Central Denmark Region Committees on Health Research Ethics, which found that the study was not considered a health research study in accordance to the Act on Research Ethics Review of Health Research Projects (Act 593 of 14 July 14 2011, Sections 14.1 and 14.2 (reference number 87/2016)). Hence, the experiment was conducted in agreement with Aarhus University's policy

for responsible conduct of research and the ethical guidelines for experiments with humans in the Declaration of Helsinki. Signed consent forms were collected for each participant, and information on the voluntarily nature of the experiment was given.

Participants

About 22 musicians forming 11 dyads were included in the dataset, with a mean age of 23.2 years (s.d. = 2.8). Participants self-reported their musical abilities as professional or semi-professional ($n = 21$), with one self-reporting as amateur.

Task and procedure

The participants were instructed to perform one out of two rhythms, a simple 4/4 rhythm at 120 beats per minute (BPM),

or the triplet of a 160 BPM 3-against-4 polyrhythm, according to instructions shown on a computer screen. Both these tasks result in an intertap interval of 500 ms. They were either tapping together with a computer metronome or with each other with bidirectional auditory coupling. The paradigm contained 200 trials of 12 s, with the first 2 s consisting of a metronome count-in. Participants were placed in the same room, yet at an angle so that no visual contact was achieved. They were instructed to tap on a MIDI pad using their right index finger and to look at a fixation cross on the computer screen during tapping while attempting to minimize other movements. The auditory stimuli were delivered using ER-2 insert earphones (Cortech Solutions), with sound levels set at a comfortable level for each participant. As we were interested in interpersonal synchronization strategies, we here only considered the 100 trials in which the participants were interacting with each other.

Behavioural results

We classified the synchronization strategies by the pattern of cross-correlation coefficients of the dyads' intertap intervals at lag -1, 0 and $+1$. We measured the average cross-correlations over all trials wherein the dyads were interacting with each other and clustered the data using Ward's clustering method. Three clusters were found to be significantly different at $\alpha < 0.05$ using a similarity profile analysis, shown in Figure 1B. Two of the clusters exhibited lag coefficient patterns compatible with mutual adaptation, whereas the third cluster exhibited the leading–leading pattern. When assessing the clusters, we categorized the participants primary instruments as either drums/percussive or harmonic/melodic and found a significant difference in the primary instruments (Fisher's exact test, $P = 0.033$) and in the dyad pairing (Fisher's exact test, $P = 0.048$), but no difference in musical experience, synchronization index nor tapping variability (Heggli *et al.*, 2019b). For the purpose of differentiating between the leading–leading and mutual adaptation synchronization strategies, we grouped the two clusters of participants exhibiting mutual adaptation together into one group (consisting of 8 dyads, hence 16 participants) and the participants exhibiting the leading–leading strategy into the second group (3 dyads, 6 participants) (see Figure 1B).

EEG data acquisition and processing

Continuous dual-EEG data were recorded from 32 scalp sites using Ag/AgCl impedance-optimized active electrodes (actiCAP, Brain Products, Germany). The electrodes were placed according to the extended international 10–20 system. Recordings were performed simultaneously from both members of each dyad using two identical BrainAmp MR amplifiers, recorded through the same software interface in order to achieve synchronized recordings (BrainVision, Brain Products, Germany). Electrode impedances were measured to <25 kOhm at start of recording. An online high-pass filter at 0.1 Hz was applied during recording, and the data were digitized at a sampling rate of 1000 Hz.

EEG data preprocessing

The EEG data were preprocessed using the MATLAB software toolbox FieldTrip (Oostenveld *et al.*, 2011). For artefact removal we first epoched all the trials from -3 s before trial start to 14 s after metronome start. We applied a band-stop filter at 50, 100 and 150 Hz to account for power line noise and a high-pass filter

at 1 Hz to remove slow drifts in the data. The data were visually inspected for each subject, and trials exhibiting clear non-cortical signals were removed. In addition, for eight subjects one or two noisy electrodes were removed (mean = 1.25 electrodes). At this point, one subject was rejected due to excessively noisy signals (time-locked abrupt amplitude changes corresponding to finger tap events were present in all electrodes, likely due to head movements). Following visual inspection, we used independent component analysis (ICA) to extract eye blink components, and identified an average of two components per participant (Jung *et al.*, 2000). After reconstructing the signal without the identified eye blink-related ICA components, we replaced any missing electrodes using the average of its neighbours and re-referenced the data to the average overall electrodes.
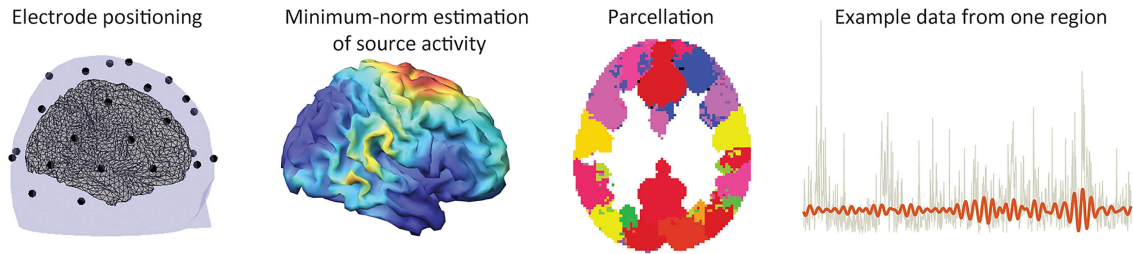
Source reconstruction

To harmonize our results with existing literature on functional connectivity and to make inferences about interacting brain regions (which cannot be done in sensor-level analysis of functional connectivity in EEG), we performed source reconstruction (Lai *et al.*, 2018). We used minimum-norm estimation in FieldTrip, using a template standard head model (Oostenveld *et al.*, 2003) and a cortical sheet with 5124 vertices (Tzourio-Mazoyer *et al.*, 2002), as illustrated in Figure 2A. The preprocessed EEG data were down-sampled to 250 Hz, and estimation was performed on a per-epoch basis with noise covariance calculated over the 400 ms prior to trial start, retaining only the data from trial start to trial end (12 s). To partly alleviate limited spatial resolution and to harmonize our analysis with existing research on functional connectivity, we parcellated source-resolved signals into 39 regions of interest (ROIs) using a parcellation template from Colclough et al. (2015). This parcellation is based on MEG-acquired resting state data and is connectivity based as opposed to anatomically based. This parcellation offers a relevant selection of regions, as well as a conservative number of ROIs which made it well suited for our low-density EEG array. Nonetheless, the limited spatial precision of the source-resolved signal should be noted. (For a list of ROIs, and their centre of gravity, see Supplementary Table 1.) This procedure was applied to each subject separately, resulting in 21 $N \times T$ matrices, with $N = 39$ representing the brain ROI and T ranging from 238 650 to 310 000 due to removal of noisy trials (161 out of a total of 2100 trials) in the preprocessing step.

Dynamic phase-locking analysis

To calculate the phase alignment between each pair of brain regions, we first filtered the data into two frequency ranges of interest, the alpha range (8–12 Hz) and the beta range (12–30 Hz), using a sixth-order Butterworth bandpass filter to achieve a steep cut-off, illustrated in Figure 2A (Sharma *et al.*, 2017; Oh *et al.*, 2018). These two frequency ranges were chosen due to their prevalence in the EEG literature considering interpersonal synchronization (Tognoli *et al.*, 2007; Babiloni *et al.*, 2012; Konvalinka *et al.*, 2014; Novembre *et al.*, 2016, 2017; Dumas *et al.*, 2019). Due to the high temporal resolution of the data, we chose a windowed approach wherein we first estimated the phases at each sample point, t, using the Hilbert transform. Following this we calculated a dynamic phase-locking matrix dPL (n_1, n_2, w), which estimates the phase alignment between brain areas n_1 and n_2 at time window w using the circular mean over 50 non-overlapping samples, as shown in Equation 1. To calculate the circular mean,
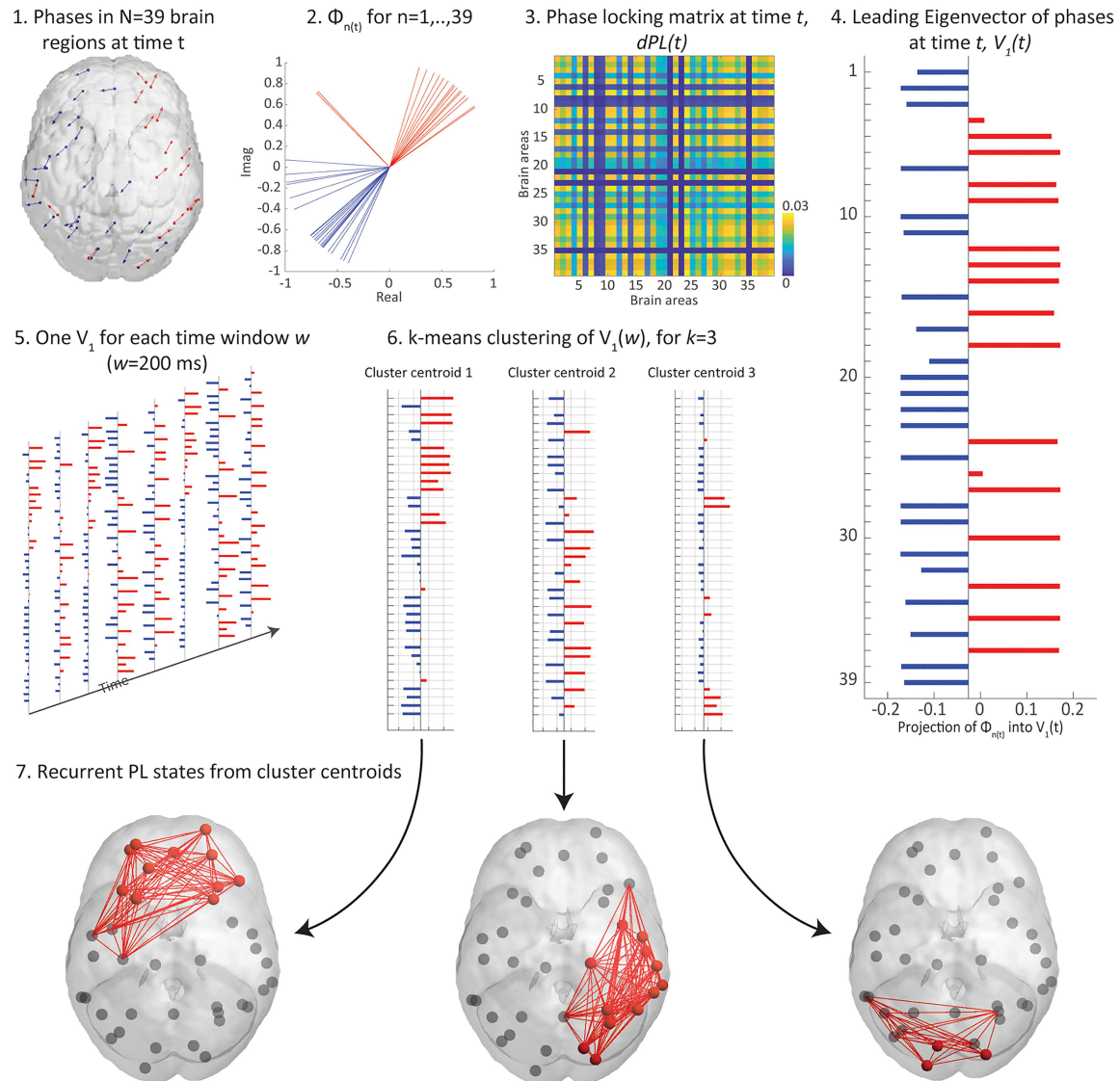
Fig. 2. In (A), the source reconstruction process is illustrated. Electrode positioning is illustrated on a template standard head model, with a cortical sheet inside. The minimum-norm estimation of source activity was parcellated into 39 brain regions, here illustrated by a horizontal section. Example data from one brain region was shown unfiltered in grey and filtered to 8–12 Hz in red. In (B), we illustrate the LEiDA analysis. In 1, the instantaneous phase at time *t* is shown for the 39 brain regions, illustrated as arrows located on the centre of gravity of each region. In 2, the phases are shown in the complex plane, and 3 shows the resulting phase-locking matrix at time *t*. The leading eigenvector, V_1, of the phase-locking matrix is shown in 4. This vector captures the main orientation of the phases at a given time, and each element corresponds to its projection into the vector, here illustrated as a bar plot. We divide the elements into two communities, with red indicating a projection that has a higher value than the mean of the eigenvector and blue indicating a value below the mean. In this study, we calculate one V_1 for each time window of 200 ms, shown in 5. The resulting V_1's is then clustered using *k*-means clustering, here shown as an example for *k* = 3 in panel 6. Each cluster is represented by a cluster centroid vector, which is considered a recurrent phase-locking pattern (PL state). In 7, we show the resulting brain network for elements in the cluster centroid which are positive in relation to the mean.

we used the CircStat toolbox in MATLAB (Berens, 2009). In comparison to the commonly used phase-locking value (PLV) which is close to 1 when there is little variation in phase difference over time, our measure reaches 1 when there is no phase difference between the two signals at a given timepoint and −1 when the phase difference is 180° (Lachaux *et al.,* 1999; Lord *et al.,* 2019). The window size of 50 samples, corresponding to 200 ms, was chosen due to the observation of fast transient brain networks occurring at this timescale in magnetoencephalography studies (Baker *et al.,* 2014; Vidaurre *et al.,* 2016):

$$dPL\,(n_1, n_2, w) = \overline{\alpha}\,(\cos\,(\theta\,(n_1, t_{1..50}) - \theta\,(n_2, t_{1..50}))) \tag{1}$$

This resulted in a three-dimensional dPL for each subject with size $N \times N \times W$, where $N = 39$ is the number of brain areas and W is the number of time windows, ranging from 4773 to 6200.

Leading eigenvector dynamics analysis

To investigate the temporal dynamics of the dPL we adapted the LEiDA method (Cabral *et al.,* 2017). Here, the leading eigenvector of the dPL is calculated for each window w, resulting in a $1 \times N$ vector capturing the main phase orientation over all regions illustrated in Figure 2B. We then calculate the mean value of the elements in the vector and divide the brain regions into two communities based on their relation to the vector mean. Using this approach, we capture the dominant connectivity pattern for each window and are able to substantially reduce the dimensionality of the data, now consisting of 120 218 vectors in total.

Phase-locking states and occurrence probability

To identify a discrete number of PL patterns, we used a k-means clustering algorithm to divide the collated PL eigenvectors into a predefined number of clusters, k. We illustrated this for $k = 3$ in Figure 2B. Here, an increase in k divides the data into increasingly finer patterns. There is as of yet no consensus on the optimal number of functional networks to consider in task-related EEG data, and we therefore chose a wide range with k ranging from 4 to 20 (Lord *et al.,* 2019). The k-means clustering algorithm was run using the squared Euclidean distance for optimization, with 50 repetitions for each k and a maximum of 200 iterations. From this clustering we obtain k cluster centroids in the shape of $1 \times N$ vectors. These vectors represent recurrent PL states found by the clustering algorithm. Subsequently, we obtain the occurrence probability for each of these PL states per k by calculating the number of windows assigned to a given PL state divided by the total number of windows, per group.

Selecting the optimal k

We assessed statistical difference in the occurrence probabilities for each single PL state between groups using a permutation-based two-sample t-test with 5000 permutations, for each level of k. Subsequently, to account for the increased chances of finding false positive due to multiple comparisons, we used a threshold wherein significance was defined as $\alpha = 0.05/k$, functioning as a per-k Bonferroni correction. As the aim of the current study was to identify differences between the two groups, we selected the k that best detected difference in occurrence probability for PL states. For the alpha frequency range, this was found for one state with $k = 13$. However, in the beta frequency range, none

of the comparisons were significant at the threshold level (see Supplementary Figure 1).

Within-network information flow analysis

While the LEiDA analysis allowed us to identify PL states containing brain networks of interest, it does not measure information flow within these networks. Furthermore, as the PL states found by LEiDA are based on decomposing the connectivity matrix using the leading eigenvector, it only finds the most prominent brain network at a given time. To better understand the activity within networks, we used phase transfer entropy (PTE) to assess the brain regions' preferred direction of information flow (Lobier *et al.,* 2014). PTE is a measure of the causal influence of a source signal on a target signal, which we calculated between all brain regions in the network of interest per trial, following the procedure described in Hillebrand *et al.,* 2016. To obtain a measure of preferred directionality, the directed PTE (dPTE), we normalized the PTE using the following equation: $dPTE_{n_1,n_2} = \frac{PTE_{n_1,n_2}}{PTE_{n_1,n_2} + PTE_{n_2,n_1}}$. Here, n_1 and n_2 are two brain regions, and PTE is the phase transfer entropy between them. The value of $dPTE_{n_1,n_2}$ ranges from 0 to 1, and when the preferred direction of information flow goes from brain region n_1 to n_2, it is bounded $0.5 < dPTE_{n_1,n_2} \leq 1$. On the other hand, if information preferentially flows from brain region n_2 to n_1, it is bounded $0 \leq dPTE_{n_1,n_2} < 0.5$. We averaged the dPTE matrix for each participant and then calculated the mean dPTE per brain region in a network of interest. To statistically quantify differences in within-network information flow between the two groups of participants, we used a permutation-based t-test with 10 000 permutations for each brain region, with FDR correction.

Results

We found significantly different between-group occurrence probabilities for one of the PL states in the alpha frequency range (PL state 3, $P = 0.0031$, $\alpha = 0.0038$, see Figure 3A). This state is characterized by a predominantly right-lateralized temporoparietal network, consisting of 13 brain regions. This network exhibits contributions from, amongst others, the right temporoparietal junction, right supramarginal gyrus, right auditory cortex, right somatosensory cortex and right middle temporal cortex and thus covers important structures related to action and perception (Zatorre *et al.,* 2007). The leading–leading group was significantly less likely to exhibit this PL state compared to the mutual adaptation group (5.12% (s.d. = 1.35) vs 6.64% (s.d. = 0.9), respectively).

The within-network analysis indicated that four regions exhibited significant difference in directionality of information flow: right somatosensory cortex (rSSC, $P = 0.0416$), right precuneus (rPCUN, $P = 0.004$), right supramarginal gyrus (rSMG, $P = 0.0389$) and right middle temporal cortex (rMTC, $P = 0.0416$). In the mutual adaptation group, the rSSC, rSMG and rMTC were predominantly transmitting information, whereas in the leading–leading group, these regions were predominantly receiving information. For the mutual adaptation group, the rPCUN was predominantly sending information, whereas in the leading–leading group, it was predominantly receiving information. These values are summarized in Table 1. The preferred direction of information flow for the regions in the network is illustrated on a cortical surface in Figure 4A, and the individual connections from each of the significant regions are illustrated for both groups in Figure 4B.

(A) Overview of PL state 3

1. Network nodes and connections

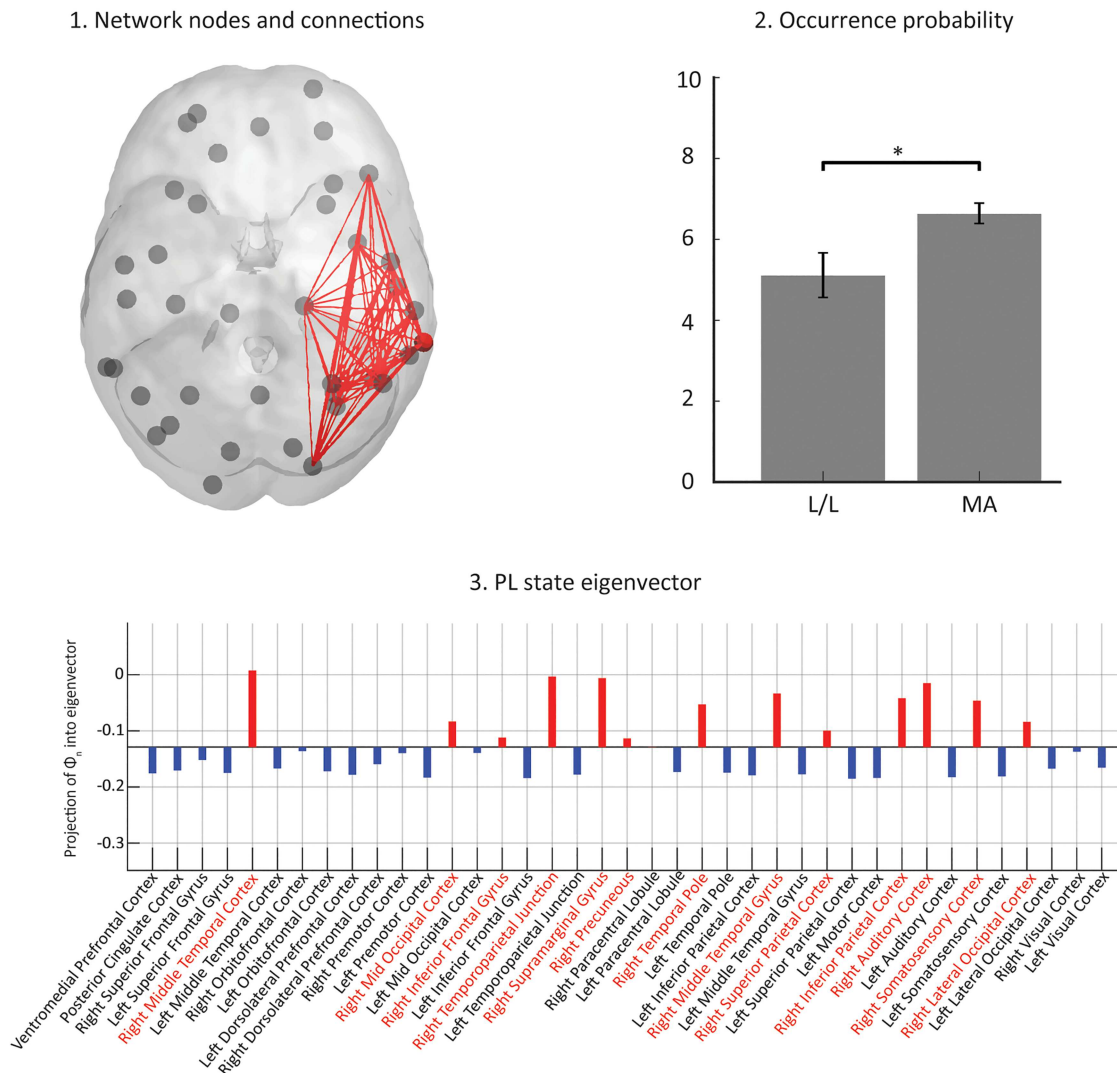### 2. Occurrence probability

3. PL state eigenvector

Fig. 3. (A) shows the PL state determined to be significantly different in occurrence probability between the group of participants exhibiting the leading–leading strategy and the group of participants using the mutual adaptation strategy. In 1, the network nodes and connections are shown, and 2 shows the occurrence probability in percent for this state. L/L indicates leading–leading and MA indicates mutual adaptation. In 3, the PL state eigenvector is shown, with red indicating regions forming the brain network.

**Table 1.** Mean dPTE for the significantly different brain regions

Region	rSSC		rPCUN		rSMG		rMTC	
	Mean	s.d.	Mean	s.d.	Mean	s.d.	Mean	s.d.
1: Leading–leading	0.5029	0.0027	0.4976	0.0023	0.5010	0.0015	0.5020	0.0027
2: Mutual adaptation	0.4995	0.0026	0.5018	0.0017	0.4975	0.0030	0.4986	0.0028

Discussion

This study is one of the first to investigate dynamical functional connectivity differentiating interpersonal interaction strategies in joint action. We found that the dyads exhibiting the mutual adaptation strategy and those exhibiting the leading–leading strategy differed both in their occurrence probability of a transient right-lateralized temporoparietal brain network and in the activity within this network. This network's primary contributors include auditory areas, motor regions, the right supramarginal gyrus and the right temporoparietal junction, as illustrated in Figure 3A. The network hence covers regions crucial for both action and perception (Zatorre et al., 2007; Burunat et al., 2017). We found that the mutual adaptation group was characterized by having a higher occurrence probability of this network as compared to leading–leading group. When analysing the information flow within the network, we find a key difference in the direction of information flow in the

(A) Information flow within PL state 3

Group 1: Leading-leading   Group 2: Mutual adaptation   Contrast: Group 1 - Group 2
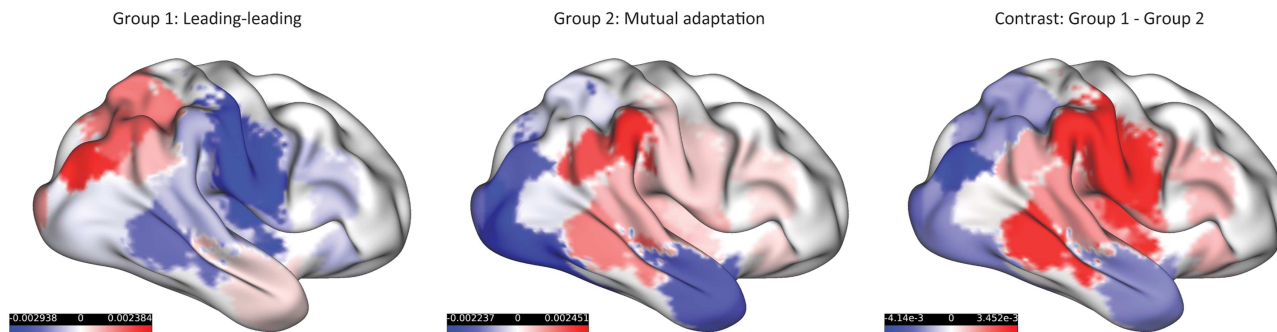
(B) Network connections within PL state 3

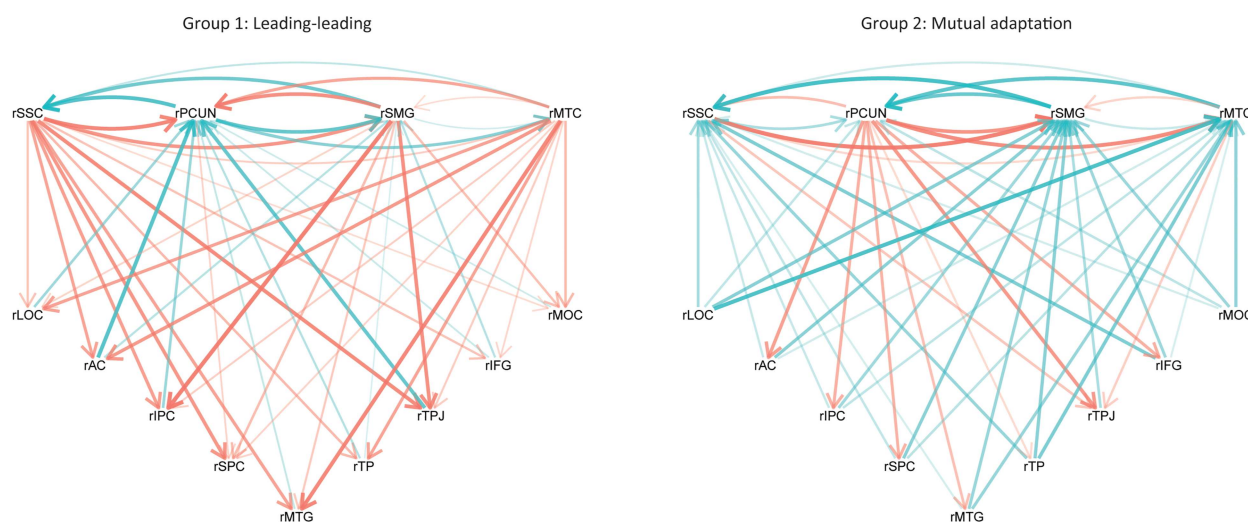Group 1: Leading-leading   Group 2: Mutual adaptation

Fig. 4. Information flow within the PL state 3 network. In (A), the information flow within this network for both synchronization strategies, as calculated with dPTE, is shown. Here, the dPTE is centred to 0, so that a positive value indicates that a brain region is predominantly sending information (shown in red) and a negative value indicates that it is predominantly receiving information (shown in blue). On the right is the contrast, calculated as Group 1 minus Group 2, with negative values in blue and positive values in red. In (B), we illustrate the network connections, considering the four regions (rSSC, rPCUN, rSMG and rMTC, shown on the top) which were significantly different in their mean dPTE between the two groups. A red line indicates information outflow, and a blue line indicates information inflow. For the four significantly different regions, we plot their relation to the remaining nine regions in the network, here shown in the staggered bottom row. In addition, we also illustrate the information flow between the four significantly different regions on the top, which are then symmetric due to the nature of dPTE.

somatosensory cortex, precuneus, supramarginal gyrus and middle temporal cortex. During mutual adaptation, the right somatosensory cortex receives information from the right auditory cortex, whereas this relationship is reversed in leading–leading, possibly indicating that the auditory perception to a lesser degree influences somatosensory perception in the leading–leading group. In mutual adaptation the right supramarginal gyrus acts as a receiving hub, whereas in leading–leading it predominantly transmits information, in particular to the right temporoparietal junction and the right inferior parietal cortex. The strongest difference is found in the right precuneus, which during leading–leading predominantly receives information, whereas it transmits information to multiple regions during mutual adaptation. One should note that the spatial resolution in our source-resolved EEG signal is limited and further studies are necessary to clarify our findings in regard to accurate locations. Nonetheless, our results suggest that mutual adaptation and leading–leading are differentiated by information flow within a transient action–perception-related functional brain network.

While the mechanisms underlying interpersonal synchronization share many similarities with physically coupled systems, the key difference is that coupling between humans is mediated via perceptual links (Koban *et al., 2017*). In addition, research indicates that merely perceiving the action of others is not sufficient for synchronization to occur, but rather, active attending is necessary (Richardson *et al., 2007*). Hence, this necessitates recruitment of brain processes underlying both action and perception during interpersonal synchronization.

Further support for our findings comes from previous work employing neurophysiological measures to investigate differences in synchronization and non-synchronized behaviour. In the previous EEG research, Tognoli et al. reported two oscillatory components termed the phi complex located above the right centroparietal cortex, a proposed measure of external influence on actions in dyadic synchronized behaviour (Tognoli *et al., 2007*). While these components were identified by their amplitude and were restricted to a narrow frequency band, their overlapping location with the network observed here is of interest. Similar findings looking at inter-brain measures report increased neural synchronization in centroparietal regions, and in particular the right parietal region, similar in topology to the network observed in our dataset (Dumas *et al., 2010, 2019*). This suggests involvement of parietal structures in synchronized behaviour, in addition to the regions and networks involved in perceiving and producing the actions

necessary for synchronization to occur. The network identified in our study displays a similar topology with these previous findings, suggesting that the difference in synchronization strategies is embedded within a brain network involved in general synchronization behaviour.

A recent theory has proposed that unintentional synchronized behaviour emerges from individual brains collectively striving for computational efficiency (Koban *et al.,* 2017). A mechanism for this is proposed to be the processes linked to self–other integration. Or, in other words, how the actions of the other are integrated or segregated with the actions produced by the self (Novembre *et al.,* 2016). During explicit interpersonal synchronization with bidirectional auditory coupling, such as in our joint finger-tapping experiment, this relates to the degree which one attributes the auditory feedback coming from the other person's tapping to one's own finger taps. Mutual adaptation, within this framework, may be a result of both participants attempting to reduce the difference between their own and the other's action (their auditory perception). When the difference between action and perception becomes sufficiently small, the participants no longer need to classify what they hear as unrelated to what they do, and thus mutual adaptation emerges, wherein the tap-by-tap adjustments are likely not consciously processed. This process is hypothesized to lead to synchronized neural representations of self and other (Koban *et al.,* 2017). In this framework, synchronization strategies can be described as resulting from the individual within the dyad either classifying the auditory feedback from the other as causally linked to the actions performed by the self or as distinct. In the case of the latter, where both dyad members segregate the auditory information from the other and the action produced by the self, a leading–leading interaction occurs (Heggli *et al.,* 2019a). Hence, in a pure leading–leading interaction, there should be no directional information flow between the actions produced by one dyad member and those from the other dyad member. This would also entail that neural representations of self and other would not be synchronized. The network identified in this work is a prime candidate for such a self–other integrating network, as it contains regions linked to functions of segregation and integration of self and other, such as the temporoparietal junction, supramarginal gyrus and precuneus, as well as action–perception-related regions (Farrer and Frith, 2002; Decety and Lamm, 2007; Lamm *et al.,* 2007; Schilbach *et al.,* 2013; Fairhurst *et al.,* 2014; Plaze *et al.,* 2015; Hoffmann *et al.,* 2016; Bolis *et al.,* 2017; Abe *et al.,* 2019).

The question then becomes why phased locking activity in this network is present in both synchronization strategies. We believe there are two likely interpretations. First, mutual adaptation is a strong attractor state in interpersonal synchronization, but it is not the only attractor state. This is shown in our behavioural results, wherein a stable synchronized interaction is maintained in the leading–leading group, and in other studies reporting a leading–following interaction (Fairhurst *et al.,* 2014; Konvalinka *et al.,* 2014; Gebauer *et al.,* 2016). However, mutual adaptation is likely the strongest attractor state due to the brain's inherent tendency towards reducing computational complexity (Koban *et al.,* 2017). It is well known that musical practice and expertise have the ability to shape brain functioning, evident even on low-level responses such as the mismatch negativity (Vuust *et al.,* 2005, 2011). The group of musicians exhibiting the leading–leading strategy in this study were distinguishable based on their primary instrument, as they consisted primarily of drummers (Heggli *et al.,* 2019b). Drummers are often expected to be the main timekeeper (Matthews *et al.,* 2016; Smith, 2016).

Hence, they need to separate their own actions from those of the other musicians in order to consciously decide whether they should adapt to their rhythmic patterns or not. It may then be that the reduced occurrence probability of the network found in this study reflects the drummers' ability to avoid falling into mutual adaptation.

The second explanation stems from the LEiDA analysis which relies on the leading eigenvector for a given time window to identify recurrent phase-locking states. This means that there likely is meaningful synchronized activity within the network we identified at more time windows than identified by the LEiDA analysis, albeit not at a strength where it gets picked up by the leading eigenvector. To address the latter, our within-network information flow analysis identified nodes in the network that differed in their directionality of information flow between the two groups.

We found four brain regions within the network that significantly differed in terms of their mean dPTE value between the two synchronization strategies, as summarized in Table 1. Of particular interest is the role of the right precuneus, which exhibits the largest difference between the two groups. In mutual adaptation the right precuneus predominantly transmits information, and in particular to the supramarginal gyrus, auditory cortex, and temporoparietal junction. This relationship is reversed in leading–leading, as illustrated in Figure 4. The precuneus has been proposed to serve an integrator of external and self-generated information, with fMRI studies showing increased activity when we consider a perceived action as linked to another agent (Farrer and Frith, 2002; Cavanna and Trimble, 2006; Chaminade *et al.,* 2012; Fairhurst *et al.,* 2014; Crafa *et al.,* 2020). While EEG-based connectivity measures cannot be directly linked to activity-based measures such as the BOLD response used in fMRI, it is nonetheless highly intriguing that the precuneus substantially changes its information flow between the two synchronization strategies.

In leading–leading the precuneus only transmits information to the right inferior parietal cortex, whereas in mutual adaptation it exhibits a more varied connectivity pattern. In the leading–leading group, we see information transfer from the somatosensory cortex to the precuneus and from the supramarginal gyrus to the precuneus. Whereas in mutual adaptation the precuneus transmits information to the supramarginal gyrus and receives information from the somatosensory cortex. A likely interpretation is that the precuneus through its role in integrating external and self-related information acts as a network synchronization moderator. For instance, if the auditory information stemming from the other is considered to be causally related to the actions produced by the self, then the precuneus allows information flow throughout the rest network leading to synchronized activity. This view is supported by resting state research indicating connectivity between the dorsal–anterior precuneus and somatomotor regions and the superior temporal gyrus (Zhang and Chiang-shan, 2012). Hence, we would propose the right precuneus is a likely candidate for the self–other integration/segregation underlying synchronization strategies. We hypothesize that in cases where the precuneus switches from a receiving to a transmitting function, one would observe increased synchronized behaviour within the right-lateralized network we identified in this study, and vice versa.

Notably, one of the main limitations of our study is the sample size, particularly of our leading–leading group (consisting of six participants). The reason for this is that this is an emergent strategy and that it only seems to emerge within dyads of

drummers, who are difficult to recruit. Follow-up studies should explicitly address differences in brain networks during dissimilar interpersonal strategies by investigating pairs of drummers *vs* pairs of other musicians.

In sum, our findings indicate that the difference between synchronization strategies is embedded in a transient action–perception network. We find that mutual adaptation and leading–leading can be distinguished by the occurrence probability of phase-locking within this network and propose that the right precuneus plays a critical role in determining the within-network dynamics. For future studies, it would be highly interesting to see whether the brain network identified here reflects dynamic changes in interpersonal synchronization strategies during an interaction. These findings are consistent with the theory that dyadic synchronization strategies depend on self–other integration and point future research towards investigating the right precuneus' role in this process.

Supplementary data

Supplementary data are available at *SCAN* online.

Author contributions

O.A.H., I.K. and P.V. designed the experiment. O.A.H. collected data and analyzed behavioural data together with I.K., M.L.K. and P.V. All authors contributed to analysis design. J.C. and M.L.K. conceptualized the LEiDA analysis, and O.A.H. adapted JC's code to work with EEG, with contributions from M.L.K., J.C. and I.K. The dPTE analysis was performed by O.A.H. with contributions from I.K. Interpretation of the results was done in collaboration between all authors. O.A.H. wrote the original draft of the manuscript, and all authors edited the manuscript. All authors discussed and interpreted the results.

Data availability

The code used in this study is under active development and is available on https://github.com/OleAd/LEiDA_EEG. The EEG data used are available upon reasonable request from O.A.H. and completion of a data sharing agreement as per Aarhus University data sharing regulations and GDPR rules.

Conflict of interest statement

The authors report no conflict of interest.

References

Abe, M.O., Koike, T., Okazaki, S., *et al.* (2019). Neural correlates of online cooperation during joint force production. *NeuroImage*, **191**, 150–61.

Babiloni, C., Buffo, P., Vecchio, F., *et al.* (2012). Brains "in concert": frontal oscillatory alpha rhythms and empathy in professional musicians. *NeuroImage*, **60**(1), 105–16.

Baker, A.P., Brookes, M.J., Rezek, I.A., *et al.* (2014). Fast transient networks in spontaneous human brain activity. *eLife*, **3**, e01867.

Berens, P. (2009). CircStat: a MATLAB toolbox for circular statistics. *Journal of Statistical Software*, **31**(10), 1–21.

Bolis, D., Balsters, J., Wenderoth, N., Becchio, C., Schilbach, L. (2017). Beyond autism: introducing the dialectical misattunement hypothesis and a Bayesian account of intersubjectivity. *Psychopathology*, **50**(6), 355–72.

Burunat, I., Tsatsishvili, V., Brattico, E., Toiviainen, P. (2017). Coupling of action-perception brain networks during musical pulse processing: evidence from region-of-interest-based independent component analysis. *Frontiers in Human Neuroscience*, **11**, 230.

Cabral, J., Kringelbach, M.L., Deco, G. (2014). Exploring the network dynamics underlying brain activity during rest. *Progress in Neurobiology*, **114**, 102–31.

Cabral, J., Vidaurre, D., Marques, P., *et al.* (2017). Cognitive performance in healthy older adults relates to spontaneous switching between states of functional connectivity during rest. *Scientific Reports*, **7**(1), 5135.

Cavanna, A.E., Trimble, M.R. (2006). The precuneus: a review of its functional anatomy and behavioural correlates. *Brain*, **129**(3), 564–83.

Chaminade, T., Marchant, J.L., Kilner, J., Frith, C.D. (2012). An fMRI study of joint action–varying levels of cooperation correlates with activity in control networks. *Frontiers in Human Neuroscience*, **6**, 179.

Cirelli, L.K., Einarson, K.M., Trainor, L.J. (2014). Interpersonal synchrony increases prosocial behavior in infants. *Developmental Science*, **17**(6), 1003–11.

Colclough, G.L., Brookes, M.J., Smith, S.M., Woolrich, M.W. (2015). A symmetric multivariate leakage correction for MEG connectomes. *NeuroImage*, **117**, 439–48.

Crafa, D., Stoddart, C.M., Makowski, C., Lepage, M., Brodeur, M.B. (2020). The impressionable social self of schizophrenia: neural correlates of self-other confusion after social interaction. Available: www.umbc.edu/philosophy/dwyer.

Decety, J., Lamm, C. (2007). The role of the right temporoparietal junction in social interaction: how low-level computational processes contribute to meta-cognition. *The Neuroscientist*, **13**(6), 580–93.

Deco, G., Jirsa, V.K., McIntosh, A.R. (2011). Emerging concepts for the dynamical organization of resting-state activity in the brain. *Nature Reviews Neuroscience*, **12**(1), 43.

Deco, G., Tononi, G., Boly, M., Kringelbach, M.L. (2015). Rethinking segregation and integration: contributions of whole-brain modelling. *Nature Reviews Neuroscience*, **16**(7), 430–9.

Dumas, G., Nadel, J., Soussignan, R., Martinerie, J., Garnero, L. (2010). Inter-brain synchronization during social interaction. *PLoS One*, **5**(8), e12166.

Dumas, G., Moreau, Q., Tognoli, E., Kelso, J.S. (2019). The human dynamic clamp reveals the fronto-parietal network linking real-time social coordination and cognition. *Cerebral Cortex*, **00**, 1–15, doi:10.1093/cercor/bhz308.

Fairhurst, M.T., Janata, P., Keller, P.E. (2014). Leading the follower: an fMRI investigation of dynamic cooperativity and leader–follower strategies in synchronization with an adaptive virtual partner. *NeuroImage*, **84**, 688–97.

Farrer, C., Frith, C.D. (2002). Experiencing oneself vs another person as being the cause of an action: the neural correlates of the experience of agency. *NeuroImage*, **15**(3), 596–603.

Fitzpatrick, P., Mitchell, T., Schmidt, R., Kennedy, D., Frazier, J.A. (2019). Alpha band signatures of social synchrony. *Neuroscience Letters*, **699**, 24–30.

Frith, C.D. (2007). The social brain? *Philosophical Transactions of the Royal Society of London B: Biological Sciences*, **362**(1480), 671–8.

Gebauer, L., Witek, M., Hansen, N.C., Thomas, J., Konvalinka, I., Vuust, P. (2014). The influence of oxytocin on interpersonal rhythmic synchronization and social bonding. *The Neurosciences and Music-V*.

Gebauer, L., Witek, M., Hansen, N., Thomas, J., Konvalinka, I., Vuust, P. (2016). Oxytocin improves synchronisation in leader-follower interaction. *Scientific Reports*, **6**, 38416.

Heggli, O.A., Cabral, J., Konvalinka, I., Vuust, P., Kringelbach, M.L. (2019a). A Kuramoto model of self-other integration across interpersonal synchronization strategies. *PLoS Computational Biology*, **15**(10), e1007422. https://doi.org/10.1371/journal.pcbi.1007422.

Heggli, O.A., Konvalinka, I., Kringelbach, M.L., Vuust, P. (2019b). Musical interaction is influenced by underlying predictive models and musical expertise. *Scientific Reports*, **9**(1), 11048.

Hillebrand, A., Tewarie, P., Van Dellen, E., *et al.* (2016). Direction of information flow in large-scale resting-state networks is frequency-dependent. *Proceedings of the National Academy of Sciences*, **113**(14), 3867–72.

Hoffmann, F., Koehne, S., Steinbeis, N., Dziobek, I., Singer, T. (2016). Preserved self-other distinction during empathy in autism is linked to network integrity of right supramarginal gyrus. *Journal of Autism and Developmental Disorders*, **46**(2), 637–48.

Hove, M.J., Risen, J.L. (2009). It's all in the timing: interpersonal synchrony increases affiliation. *Social Cognition*, **27**(6), 949–60.

Jung, T.-P., Makeig, S., Humphries, C., *et al.* (2000). Removing electroencephalographic artifacts by blind source separation. *Psychophysiology*, **37**(2), 163–78.

Koban, L., Ramamoorthy, A., Konvalinka, I. (2017). Why do we fall into sync with others? *Interpersonal synchronization and the brain's optimization principle. Social Neuroscience*, **14**(1), 1–9.

Konvalinka, I., Roepstorff, A. (2012). The two-brain approach: how can mutually interacting brains teach us something about social interaction? *Frontiers in Human Neuroscience*, **6**, 215.

Konvalinka, I., Vuust, P., Roepstorff, A., Frith, C.D. (2010). Follow you, follow me: continuous mutual prediction and adaptation in joint tapping. *The Quarterly Journal of Experimental Psychology*, **63**(11), 2220–30.

Konvalinka, I., Bauer, M., Stahlhut, C., Hansen, L.K., Roepstorff, A., Frith, C.D. (2014). Frontal alpha oscillations distinguish leaders from followers: multivariate decoding of mutually interacting brains. *NeuroImage*, **94**, 79–88.

Kung, S.-J., Chen, J.L., Zatorre, R.J., Penhune, V.B. (2013). Interacting cortical and basal ganglia networks underlying finding and tapping to the musical beat. *Journal of Cognitive Neuroscience*, **25**(3), 401–20.

Lachaux, J.P., Rodriguez, E., Martinerie, J., Varela, F.J. (1999). Measuring phase synchrony in brain signals. *Human Brain Mapping*, **8**(4), 194–208.

Lai, M., Demuru, M., Hillebrand, A., Fraschini, M. (2018). A comparison between scalp-and source-reconstructed EEG networks. *Scientific Reports*, **8**(1), 12269.

Lamm, C., Fischer, M.H., Decety, J. (2007). Predicting the actions of others taps into one's own somatosensory representations—a functional MRI study. *Neuropsychologia*, **45**(11), 2480–91.

Lobier, M., Siebenhühner, F., Palva, S., Palva, J.M. (2014). Phase transfer entropy: a novel phase-based measure for directed connectivity in networks coupled by oscillatory interactions. *NeuroImage*, **85**, 853–72.

Lord, L.-D., Expert, P., Atasoy, S., *et al.* (2019). Dynamical exploration of the repertoire of brain networks at rest is modulated by psilocybin. *NeuroImage*, **199**, 127–42.

Matthews, T.E., Thibodeau, J.N., Gunther, B.P., Penhune, V.B. (2016). The impact of instrument-specific musical training on rhythm perception and production. *Frontiers in Psychology*, **7**, 69.

Milward, S.J., Sebanz, N. (2016). Mechanisms and development of self–other distinction in dyads and groups. *Philosophical Transactions of the Royal Society, B: Biological Sciences*, **371**(1686), 20150076.

Novembre, G., Sammler, D., Keller, P.E. (2016). Neural alpha oscillations index the balance between self-other integration and segregation in real-time joint action. *Neuropsychologia*, **89**, 414–25.

Novembre, G., Knoblich, G., Dunne, L., Keller, P.E. (2017). Interpersonal synchrony enhanced through 20 Hz phase-coupled dual brain stimulation. *Social Cognitive and Affective Neuroscience*, **12**(4), 662–70.

Oh, S.L., Hagiwara, Y., Raghavendra, U., *et al.* (2018). A deep learning approach for Parkinson's disease diagnosis from EEG signals. *Neural Computing and Applications*, 1–7.

Oostenveld, R., Stegeman, D.F., Praamstra, P., van Oosterom, A. (2003). Brain symmetry and topographic analysis of lateralized event-related potentials. *Clinical Neurophysiology*, **114**(7), 1194–202.

Oostenveld, R., Fries, P., Maris, E., Schoffelen, J.-M. (2011). FieldTrip: open source software for advanced analysis of MEG, EEG, and invasive electrophysiological data. *Computational Intelligence and Neuroscience*, **2011**, 1.

Plaze, M., Mangin, J.-F., Paillère-Martinot, M.-L., *et al.* (2015). "Who is talking to me?"—self–other attribution of auditory hallucinations and sulcation of the right temporoparietal junction. *Schizophrenia Research*, **169**(1–3), 95–100.

Redcay, E., Schilbach, L. (2019). Using second-person neuroscience to elucidate the mechanisms of social interaction. *Nature Reviews Neuroscience*, **20**(8), 495–505.

Richardson, M.J., Marsh, K.L., Isenhower, R.W., Goodman, J.R., Schmidt, R.C. (2007). Rocking together: dynamics of intentional and unintentional interpersonal coordination. *Human Movement Science*, **26**(6), 867–91.

Sänger, J., Müller, V., Lindenberger, U. (2013). Directionality in hyperbrain networks discriminates between leaders and followers in guitar duets. *Frontiers in Human Neuroscience*, **7**, 234.

Schilbach, L., Timmermans, B., Reddy, V., *et al.* (2013). Toward a second-person neuroscience. *Behavioral and Brain Sciences*, **36**(4), 393–414.

Schilbach, L., Derntl, B., Aleman, A., *et al.* (2016). Differential patterns of dysconnectivity in mirror neuron and mentalizing networks in schizophrenia. *Schizophrenia Bulletin*, **42**(5), 1135–48.

Schmidt, R., Nie, L., Franco, A., Richardson, M.J. (2014). Bodily synchronization underlying joke telling. *Frontiers in Human Neuroscience*, **8**, 633.

Sharma, M., Dhere, A., Pachori, R.B., Acharya, U.R. (2017). An automatic detection of focal EEG signals using new class of time–frequency localized orthogonal wavelet filter banks. *Knowledge-Based Systems*, **118**, 217–27.

Smith, G.D. (2016). *I Drum, Therefore I Am: Being and Becoming a Drummer*, Routledge.

Stupacher, J., Maes, P.-J., Witte, M., Wood, G. (2017a). Music strengthens prosocial effects of interpersonal synchronization–if you move in time with the beat. *Journal of Experimental Social Psychology*, **72**, 39–44.

Stupacher, J., Wood, G., Witte, M. (2017b). Synchrony and sympathy: social entrainment with music compared to a metronome. *Psychomusicology: Music, Mind & Brain*, **27**(3), 158.

Tognoli, E., Lagarde, J., DeGuzman, G.C., Kelso, J.S. (2007). The phi complex as a neuromarker of human social coordination. *Proceedings of the National Academy of Sciences*, **104**(19), 8190–5.

Tzourio-Mazoyer, N., Landeau, B., Papathanassiou, D., *et al*. (2002). Automated anatomical labeling of activations in SPM using a macroscopic anatomical parcellation of the MNI MRI single-subject brain. *NeuroImage*, **15**(1), 273–89.

van Ulzen, N.R., Lamoth, C.J., Daffertshofer, A., Semin, G.R., Beek, P.J. (2008). Characteristics of instructed and uninstructed interpersonal coordination while walking side-by-side. *Neuroscience Letters*, **432**(2), 88–93.

Vidaurre, D., Quinn, A.J., Baker, A.P., Dupret, D., Tejero-Cantero, A., Woolrich, M.W. (2016). Spectrally resolved fast transient brain states in electrophysiological data. *NeuroImage*, **126**, 81–95.

Vuust, P., Pallesen, K.J., Bailey, C., *et al*. (2005). To musicians, the message is in the meter pre-attentive neuronal responses to incongruent rhythm are left-lateralized in musicians. *NeuroImage*, **24**(2), 560–4.

Vuust, P., Brattico, E., Glerean, E., *et al*. (2011). New fast mismatch negativity paradigm for determining the neural prerequisites for musical ability. *Cortex*, **47**(9), 1091–8.

Young, S.N. (2008). The neurobiology of human social behaviour: an important but neglected topic. *Journal of psychiatry & neuroscience: JPN*, **33**(5), 391.

Zatorre, R.J., Chen, J.L., Penhune, V.B. (2007). When the brain plays music: auditory–motor interactions in music perception and production. *Nature Reviews Neuroscience*, **8**(7), 547.

Zhang, S., Chiang-shan, R.L. (2012). Functional connectivity mapping of the human precuneus by resting state fMRI. *NeuroImage*, **59**(4), 3548–62.